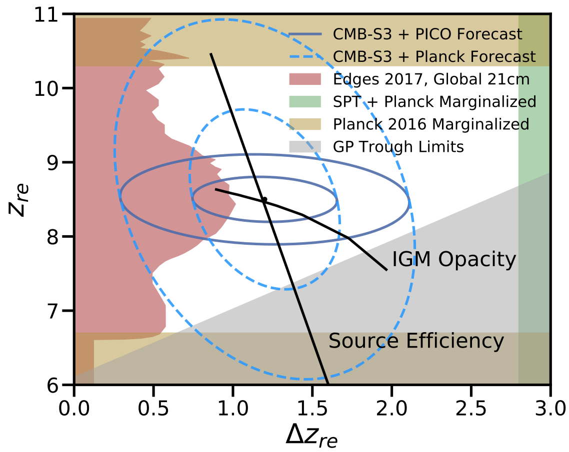

Figure 0.1: Contours of 1σ and 2σ constraints on the mean redshift and duration of reionization using PICO and CMB-S3 data (solid dark blue), and comparison with *Planck* and CMB-S3 (dash light blue). Source efficiency and IGM opacity (dark lines) are two physical parameters controlling the reionization process in current models. The PICO measurements, together with higher-resolution data of the kSZ effect, will significantly constrain the range of models allowed. We also include other constraints from *Planck*, EDGES, the Gunn–Peterson (GP) trough, and *Planck* + the South Pole Telescope [**? ? ? ?**].

0.0.1 The Formation of the First Luminous Sources

A few hundred million years after the Big Bang, the neutral hydrogen gas permeating the Universe was reionized by photons emitted by the first luminous sources to have formed. The nature of these sources and the exact history of this epoch are key missing links in our understanding of structure formation (SO5).

The reionization of the Universe imprints multiple signals in the temperature and polarization of the CMB. In polarization, the most important signature is an enhancement in the EE power spectrum at large angular scales $\ell \lesssim 10$ (Fig. **??**). This signal gives a direct measurement of the optical depth to the reionization epoch τ and thus to the mean redshift of reionization $z_{\rm re}$, with very little degeneracy with other cosmological parameters (Fig. 1).[1] *Planck*'s determination of the optical depth to reionization $\tau = 0.054 \pm 0.007\,(1\sigma)$ has indicated that reionization concluded by $z \sim 6$, but the measurement uncertainty leaves many unanswered questions including: were the ionizing sources primarily star-forming galaxies or more exotic sources such as supermassive black holes or annihilating dark matter? What was the mean free path of ionizing photons during this epoch? What was the efficiency with which such photons were produced by ionizing sources? Did the reionization epoch extend to $z \sim 15$–20, as has been claimed recently [**?**]? With ten independent maps of the entire sky, multiple frequency bands and ample sensitivity to remove foregrounds, PICO is uniquely suited to make the low ℓ EE-spectrum measurements, reach cosmic-variance-limited precision with $\sigma(\tau) = 0.002$, settle some of these questions, and significantly constrain the others (SO5).

Figure 1 presents forecasts for reionization constraints in the $z_{\rm re} - \Delta z_{\rm re}$ parameter space. These are obtained from PICO's measurement of τ in combination with S3 experiments' measurements of the "patchy" kinematic Sunyaev–Zeldovich (kSZ) effect, due to the peculiar velocities of free-electron bubbles around ionizing sources [**?**]. The figure includes curves of constant efficiency of production of ionizing photons in the sources, and of intergalactic-medium opacity, two parameters that quantify models of reionization. The curves shown are illustrative; families of models, that would be represented by parallel 'source efficiency' and 'IGM Opacity' lines, are allowed by current data. PICO's data will give simultaneous constraints on these physical parameters, yielding important information on the nature of the first luminous sources. For example, galaxies and quasars predict significantly different values for their IGM opacities and source efficiencies.

The process of reionization leaves specific non-Gaussian signatures in the CMB. In particular, patchy reionization induces non-trivial 4-point functions in both temperature and polarization [**? ?**]. The temperature 4-point function can be used to separate reionization and late-time kSZ contributions. Combinations of temperature and polarization data can be used to build quadratic estimators for reconstruction of the patchy τ field, analogous to CMB lensing reconstruction (§ **??**). These estimators generally require high angular resolution, but also rely on foreground-cleaned CMB maps. Data from PICO's high-frequency bands – which have better than 2 arcmin resolution and cover frequencies that are not suitable for observations from the

[1] The mean redshift to reionization is the redshift when 50% of the cosmic volume was reionized.

ground – will enable these estimators to be robustly applied to high-resolution ground-based CMB data, a strong example of ground-space complementarity.

Decreasing the uncertainty on τ is important to break the degeneracy between this parameter and the amplitude of the primordial power spectrum A_s, a degeneracy in the CMB power spectra that hinders all cosmological observables of the growth of structure (§ **??**). The degeneracy can only be broken through measurements of the low-ℓ EE power spectrum. PICO's cosmic-variance-limited polarization measurements will thus improve constraints on the sum of neutrino masses, dark energy, and modified gravity coming from all low-z growth measurements including galaxy lensing, velocity-field measurements, redshift-space distortions, and galaxy surveys.

0.0.2 Probing the Evolution of Structures via Gravitational Lensing and Cluster Counts

The particle content of the Universe, gravitational collapse, the effects of dark energy, and energetic feedback processes that recycle energy determine the evolution of structures in the Universe. The amplitude of linear fluctuations as a function of redshift, parameterized by $\sigma_8(z)$, is thus a sensitive probe representing the effects of physical processes affecting growth. **CMB!** (**CMB!**) photons are affected by, and thus probe, $\sigma_8(z)$ as they traverse the entire Universe. PICO will tightly constrain $\sigma_8(z)$ through measurements of gravitational lensing and cluster counts.

• **Gravitational Lensing** Matter between us and the last-scattering surface deflects the path of photons through gravitational lensing, imprinting the three-dimensional matter distribution across the volume of the Universe onto the CMB maps. The specific quantity being mapped by the data is the projected gravitational potential ϕ that is lensing the photons. From the lensing map, which receives contributions from all redshifts between us and the CMB, with the peak of the distribution at $z \sim 2$, we infer the angular power spectrum $C_L^{\phi\phi}$ (Fig. 2). Both the temperature and polarization maps of the CMB, and by extension the angular power spectra, are affected by lensing.

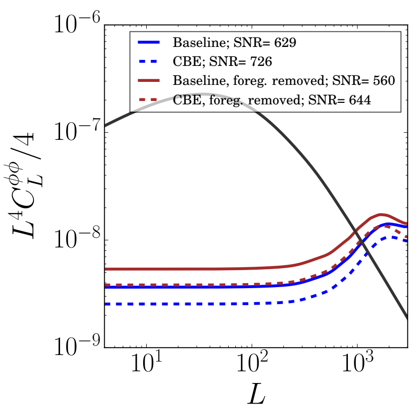

Figure 0.2: PICO will make a high **SNR!** full-sky map of the projected gravitational potential ϕ due to all matter between us and the last scattering surface at all angular scales $2 \leq L \lesssim 1000$ (Footnote **??**) for which its noise (red and blue) is below the theoretically predicted power spectrum $C_L^{\phi\phi}$ (black). Noise predictions as a function of L and anticipated **SNR!** values for the measurement of $C_L^{\phi\phi}$ are given for the baseline (solid) and CBE (dashed) cases, and without (blue) and with (red) a process of foregrounds separation, which degrades the **SNR!** by $\sim$10 %.

Planck's ϕ map had **SNR!** of $\sim$1 per L mode over a narrow range of scales, $30 < L < 50$. PICO will make a true map, with **SNR!** $\gg 1$ for each mode in the range $2 \leq L \lesssim 1000$. While *Planck* had an **SNR!** of 40 integrated across the entire $C_L^{\phi\phi}$ power spectrum [**?**], PICO will give **SNR!** of 560 and 644 for the baseline and CBE configurations, respectively; both values already account for foreground separation (Fig. 2).

PICO's ϕ map is a key ingredient in the delensing process that improves constraints on r (§ **??**) and in extracting neutrino mass constraints (§ **??**). It will also be used to constrain the properties of quasars and other high-redshift astrophysics. For example, cross-correlations with quasar samples from DESI will yield a precise determination of the quasar bias (and hence host halo mass) as a function of the quasar properties, such as (non-)obscuration. Such studies are not possible with any other lensing techniques, due to their sensitivity to lower redshifts.

• $\sigma_8(z)$ **from Gravitational Lensing** Cross-correlations between the PICO lensing-potential map and wide-field samples of galaxies and quasars provide a powerful technique to measure the time dependence of the amplitude of matter fluctuations $\sigma_8(z)$ in tomographic redshift bins. This is achieved by overcoming

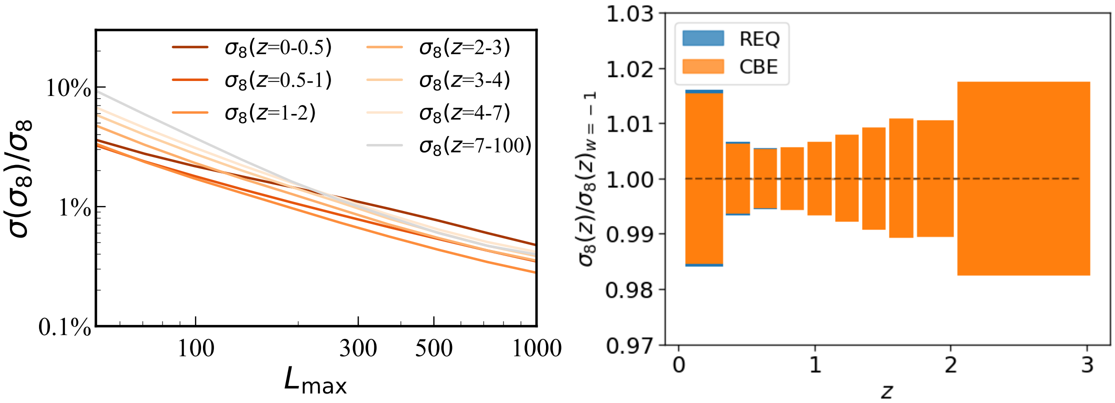

Figure 0.3: Sub-percent constraints on the evolution of σ_8 as a function of redshift will come from two independent PICO products: Correlations between PICO's deep gravitational lensing map (Fig. 2) and LSST's gold sample of galaxies (left) and cluster counts (right). Fractional uncertainties in σ_8 relative to fiducial ΛCDM values are given as a function of the finest angular scale $L_{\rm max}$ of the correlation analysis for seven redshift bins (left). The baseline and CBE configurations give essentially the same fractional errors of $\sigma_8(z)$ using cluster counts (right). LSST assumptions: 10 years, 50% sky fraction, 55 galaxies per arcmin^2 at redshift $z < 3$ with magnitude limit $i < 25.3$ [**?**], and dropout galaxies at $z > 3$ [**?**] extrapolating recent Hyper Suprime-Cam observations [**? ? ?**], with linear bias $b(z) = 1+z$.

the limitations of auto-correlations of these data sets: The lensing ϕ map is sensitive to the projection of all matter back to the last scattering surface, so it cannot resolve the time dependence of fluctuations, while galaxies and quasars trace matter in an unknown biased way so that the matter amplitude cannot be determined. Cross-correlations of the two data sets, broken down to several tomographic redshift bins, will constrain how galaxies in each bin trace the dark matter, which will yield strong constraints on $\sigma_8(z)$ and thereby on structure formation and models of dark energy and modified gravity [**? ?**].

In Fig. **??** we show projected 1σ errors on $\sigma_8(z)$ when using cross-correlations with LSST's gold sample of galaxies [**?**]. Sub-percent accuracy is obtainable with PICO's resolution which will give information extending to $L = 1000$.[2] This accuracy will be used to constrain dark energy or modified gravity, in the context of specific models, and to give a neutrino mass constraint that is independent from and competitive with that inferred from the CMB lensing auto-power spectrum (§ **??**) [**?**] .

• **Cluster Counts** The distribution of galaxy clusters in redshift is one consequence of the evolution of structures and is thus a sensitive measure of $\sigma_8(z)$. The observational quantity of interest is $dN/(dz\,dm)$, the number of observed clusters per redshift and per mean mass, from which constraints on $\sigma_8(z)$ can be derived. Galaxy clusters found by PICO via the **tSZ!** (**tSZ!**) effect (§ **??**) provide a catalog with a selection function that is simple to model and thus straightforward to use for cosmological inference. PICO's catalog will provide all clusters with masses above $\sim 3\times10^{14} M_\odot$ out to redshifts $z \sim 3$, as long as the clusters have started to virialize. We forecast that PICO will find ∼150,000 galaxy clusters, assuming the cosmological parameters from *Planck* and using the 70% of sky not obscured by the Milky Way. Redshifts will be provided by future optical and infrared surveys. Cluster masses will be inferred by optical weak lensing for clusters with $z < 1.5$ and by PICO's own CMB halo lensing data at higher redshifts (see next paragraph). The catalog will give the most massive clusters over the full sky. Sub-percent determination of σ_8 will be provided with this catalog for $0.5 < z < 2$ (Fig. **??**), and a neutrino mass constraint of 14 meV that is independent from the one coming from the lensing measurements (SO3, § **??**).

Calibrating the masses of clusters, that is determining $m(z)$, is the most uncertain step in inferring σ_8 and other cosmological parameters using cluster counts. PICO will provide calibration using 'CMB halo lensing', an approach that uses the small-scale effects of gravitational lensing due to dark matter halos around clusters and proto-clusters [**? ? ?**]. The technique is particularly effective for measuring halo masses out to high redshifts where gravitational lensing of background objects no longer works because there are no

[2] PICO's resolution is sufficient to give information for $L > 1000$, but at these scales structures are non-linear and will not be used to constrain $\sigma_8(z)$.

background sources. The approach is illustrated in Fig. 5, which gives the 1σ uncertainty in a halo mass measurement as a function of the object's redshift. PICO will measure the mass of individual low-mass clusters ($\sim 10^{14}\,\mathrm{M}_\odot$) over a wide redshift range, and by stacking will determine the mean mass of smaller halos, with masses of $\sim 10^{13}\,\mathrm{M}_\odot$, which include those hosting individual galaxies. Because the vast majority of clusters have masses that are larger than $\sim 10^{14}\,\mathrm{M}_\odot$, the PICO data will provide mass calibration for all objects of interest. The flattening at high redshift reflects the fact that the technique is sensitive over a broad range of redshifts. The high-frequency PICO data, for which the resolution matches ground-based instruments' resolution at lower frequencies, will play an essential role in cleaning foregrounds, particularly those derived from the temperature-based estimator, which is most contaminated by foregrounds.

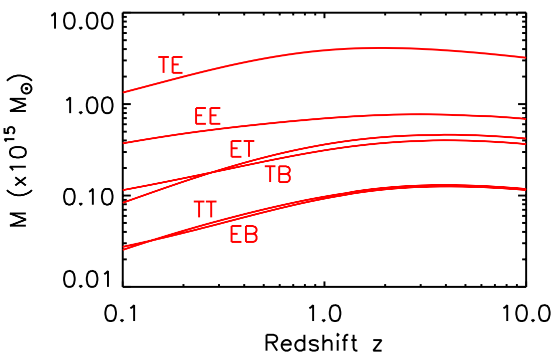

Figure 0.4: PICO will provide mass calibration for individual clusters and proto-clusters with mass as low as $10^{14} M_\odot$ at $z > 2$ using 'halo lensing'. Curves for different CMB signal correlations (red) give the 1σ sensitivity of an optimal mass filter [?] as a function of z. The curves are flat at high redshift, demonstrating that the technique probes a broad range of redshifts. For PICO, the EB and TT estimators are equivalent, offering important cross-validation of measurements because the systematics are very different for temperature and polarization.

Beyond its role in calibrating masses for cluster counts, PICO's halo lensing measurements will also be a unique tool for measuring the relation between galaxies and their dark matter halos during the key epochs of cosmic star formation at $z \geq 2$, which is not reachable by other means. This will provide valuable insight into the role of environment on galaxy formation during the rise to and fall from the peak of cosmic star formation at $z \sim 2$.

0.0.3 Constraining Feedback Processes through the Sunyaev–Zeldovich Effect

Not all CMB photons propagate through the Universe freely; about 6% are Thomson-scattered by free electrons in the **IGM!** (**IGM!**) and **ICM!** (**ICM!**). These scattering events leave a measurable imprint on **CMB!** temperature fluctuations, which thereby contain a wealth of information about the growth of structures and the thermodynamic history of baryons. A fraction of these photons are responsible for the thermal and kinetic Sunyaev–Zeldovich effects (tSZ and kSZ) [? ?]. The amplitudes of the tSZ and kSZ signals are proportional to the integrated electron pressure and momentum along the line of sight, respectively. They thus contain information about the thermodynamic properties of the **IGM!** and **ICM!**, which are highly sensitive to astrophysical feedback. Feedback is the process of energy injection into the **IGM!** and **ICM!** from accreting supermassive black holes, supernovae, stellar winds, and other sources. Feedback processes are the most uncertain, yet crucial, ingredient in modern theories of galaxy formation; they are required in order to match observations of the stellar properties of galaxies, but the underlying details of the physical processes involved are still highly uncertain.

Multifrequency **CMB!** data also allow the reconstruction of full-sky 'Compton-y maps'of the tSZ signal. With low noise and broad frequency coverage, which is essential for separating out other signals, PICO will yield a definitive Compton-y map over the full sky, with a total **SNR!** of 1270 for the CBE and $\approx 10\%$ lower for the baseline configurations (Fig. 6). This is nearly two orders of magnitude higher **SNR!** than *Planck*, which already gave data with much higher **SNR!** than ground-based experiments. The tens of thousands of clusters forecast to be detected by PICO will be found in the y map (§ **??**).

Strong constraints on models of astrophysical feedback will be obtained from the analysis of the PICO y-map, both from its auto-power spectrum and from cross-correlations with galaxy, group, cluster, and quasar samples. As an example, we forecast the detection of cross-correlations between the PICO y-map and galaxy weak-lensing maps constructed from LSST and WFIRST data. Considering the LSST gold weak-lensing

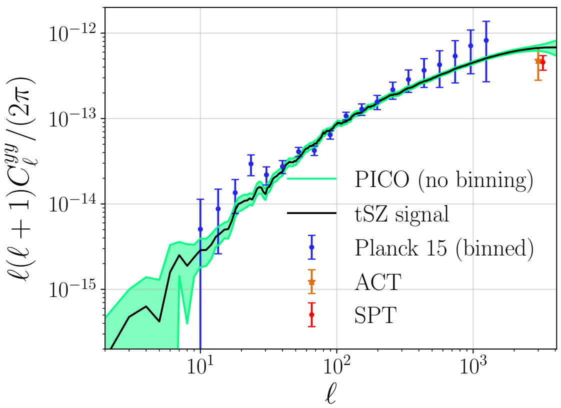

Figure 0.5: The PICO y-map will give a tSZ power spectrum with an **SNR!** of 1270 (green, 1σ per ℓ mode), which is nearly 100 times larger than from *Planck* (blue). Binning the data (not shown) as was done for *Planck* would further increase the **SNR!**. We include current measurements by the ground-based SPT and ACT [**?** **?**]. In these forecasts we reconstruct the Compton-y field from maps that include Galactic foregrounds, CMB fluctuations, and PICO CBE noise using the needlet internal linear combination algorithm [**?**]. The input maps use the *Planck* sky model [**?**].

sample, with a source density of 26 galaxies/arcmin^2 covering 40% of the sky, we forecast a detection of the tSZ–weak-lensing cross-correlation with **SNR!** = 3000. Cross-correlations with the galaxies themselves will be measured at even higher **SNR!**. At this immense significance, the signal can be broken down into dozens of tomographic redshift bins, precisely tracing the evolution of thermal pressure over cosmic time. For PICO and WFIRST (assuming 45 galaxies/arcmin^2 covering 5.3% of the sky), we forecast **SNR!** = 1100 for the tSZ-weak lensing cross-correlation. The WFIRST galaxy sample extends to higher redshift, and thus this high-**SNR!** measurement will allow the evolution of the thermal gas pressure to be probed to $z \approx 2$ (the peak of the cosmic star formation history) and beyond. These measurements will revolutionize our understanding of galaxy formation and evolution by distinguishing between models of feedback energy injection at high significance. Additional cross-correlations of the PICO y-map with quasar samples, filament catalogs, and other large-scale structure tracers will provide valuable information on baryonic physics that is complementary to inferences from the lensing cross-correlations described earlier.